TRABAJO DE FIN DE GRADO:

Whispering Gallery Modes temperature sensor using a holmium doped glass microsphere

Autora:

Laura Marina de Sousa Vieira

Tutores:

Inocencio Rafael Martín Benenzuela

Susana Ríos Rodríguez

Grado en Física

Universidad de La Laguna

Index

Resumen

El objetivo principal de este trabajo es estudiar la utilidad de microesferas vítreas dopadas con iones trivalentes de holmio como sensores ópticos de temperatura. Las microesferas son cavidades resonantes de diámetros del orden de micras, fabricadas de un material dieléctrico transparente que debe tener un índice de refracción mayor que el del medio que las rodea. Cuando un haz de luz incide sobre una microesfera, este puede quedar atrapado en ella por reflexión total interna. En el interior de la esfera se producen una serie de reflexiones, algunas de las cuales pueden llegar a su punto inicial en fase, lo que produce un efecto de resonancia. Dichas resonancias se conocen como "Whispering Gallery Modes". Estos modos resonantes son muy sensibles a variaciones en el entorno de la microesfera, por ejemplo, un cambio en la temperatura de la microesfera produce alteraciones en su tamaño (debido a la dilatación térmica) y en su índice de refracción. Estos cambios inducen desplazamientos en las longitudes de onda resonantes.

En este trabajo, las microesferas utilizadas están dopadas con iones trivalentes de holmio. En este caso, cuando se excita la microesfera con un láser, se producen las emisiones de los iones de holmio. Algunas de las longitudes de onda de dichas emisiones pueden quedar atrapadas y resonar dentro de la microesfera, si cumplen la condición de resonancia. Si se lleva a cabo la excitación en el centro de la esfera y la detección en su borde, es posible observar los "Whispering Gallery Modes" como picos estrechos, superpuestos a las bandas anchas de emisión del holmio. Estos picos muestran un desplazamiento al rojo cuando tiene lugar un cambio en la temperatura de la microesfera. Por tanto, si se obtienen los espectros de emisión para diferentes temperaturas de la microesfera dopada con Ho^{3+}, se puede obtener el desplazamiento de dichos picos con la temperatura. Esta calibración permite estimar la temperatura de una microesfera que se ha calentado al ser excitada mediante un láser a una determinada potencia, a partir del desplazamiento de sus modos resonantes.

Chapter 1. Introduction.

Hoy en día, los sensores ópticos son ampliamente utilizados debido a sus múltiples ventajas frente a los sensores tradicionales. Específicamente, las microesferas se utilizan como sensores de temperatura, ya que sus modos resonantes, conocidos como "Whispering Gallery Modes", son muy sensibles ante un cambio de temperatura. El objetivo principal de este trabajo es estudiar la posibilidad de utilizar microesferas vítreas dopadas con iones trivalentes de holmio como sensores de temperatura. Cabe destacar que el holmio tiene una banda de emisión aproximadamente en 1200 nm, que cae dentro de la segunda ventana biológica, lo que resulta interesante en el campo de la medicina.

A microsphere consists on a spherical resonator that presents morphology dependent resonances. It is usually made of a transparent dielectric that must have a higher refractive index than the surrounding media, to produce total internal reflection. These resonators can reach high-quality factors, in the range of 10^7 to 10^9 [1, 2], because of their minimal reflection losses and their very low material absorption, leading to a very high energy density [3].

The resonances supported by microspheres are known as Whispering Gallery Modes (WGM). The study of the WGM started at the beginning of the 20th century when Lord Rayleigh [4] studied the propagation of the sound over a curved gallery surface [5, 6]. Moreover, the equations for resonant wavelengths of dielectric spheres were obtained by Debye in 1909 [7], and also, can be deduced from the studies by Mie in 1908, on his paper about the scattering of plane electromagnetic waves by spheres [8]. On the other hand, the earliest observations of WGM in optics were done with solid state WGM lasers. Using Sm:CaF_2 crystalline resonators with a millimetric size, laser action was studied [9]. In the early 1980s, the utility of WGM to measure the size, shape, temperature, or refractive index of a spherical particle was demonstrated [10, 11].

Nowadays, WGM spherical resonators have a wide range of applications. For example, as temperature sensors [12, 13], applications in medicine [14], laser fabrication [15]. Another application is to use microspheres as chemical vapor sensors. Miaomiao *et*

al. [16] fabricated organic WGM resonators and, by measuring the shift on the lasing modes when they are exposed to an organic vapor, they successfully monitored the variation on the concentration of the chemical gas.

Currently, microspheres are extensively used as optical sensors. The fundamentals of optical sensing devices are to analyse the change in the intensity of light beams, or changes in their phases, as they interact with a physical system. These devices present numerous advantages compared to traditional sensors, in terms of electrical passiveness, greater sensitivity, freedom from electromagnetic interference, wide dynamic range, point and distributed configurations and multiplexing capabilities [17]. Another benefit of using microspheres as optical sensors is that the detection can be carried out remotely, so it is possible to make measurements inside the system causing just a small perturbation in the physical system [18].

Specifically, microspheres are useful as temperature sensors [12, 13] because of the high sensitivity of their resonance modes (WGM) to any change of temperature. As it will be discussed later, the wavelengths of the WGM can be shifted if there is a change in the microsphere size or in the optical properties of the surrounding medium, for example due to a temperature variation. So, monitoring the shift in the WGM peaks when a temperature change takes place, the temperature of the microsphere can be estimated.

An interesting glass to fabricate microspheres is yttrium aluminosilicate: Y_2O_3–Al_2O_3–SiO_2, known as YAS, because it has application in medicine. This type of microspheres has been used to treat liver cancer [19, 20]. One way to treat malignant tumours is with radiation, but external radiation doses are limited because they damage the nearby healthy tissue. An interesting solution to this issue is to place the radiation source inside the tumour. Radioactive microspheres can be injected into the tumour [20].

On the other hand, microspheres are usually doped with lanthanides because these elements have numerous fluorescent emissions in the visible and the near infrared region of the electromagnetic spectrum [21]. The triple ionized holmium ions have an emission peak at about 1200 nm [22], that corresponds to the $^5I_6 \rightarrow {}^5I_8$ transition, in the near infrared region. This emission is interesting because it lays in the second biological window, that extends from 1000 nm to 1400 nm, where the absorption of light by the constituents of biological tissue is minimized, i.e. tissues are partially transparent [23]. Two water

absorption bands located at about 980 nm and 1500 nm limit this spectral range [24]. This window can be observed in Fig. 1, where the absorption curves for human fat and water are shown. Multiple researches relating the second biological window are being carried out for medical and biological applications [23-27].

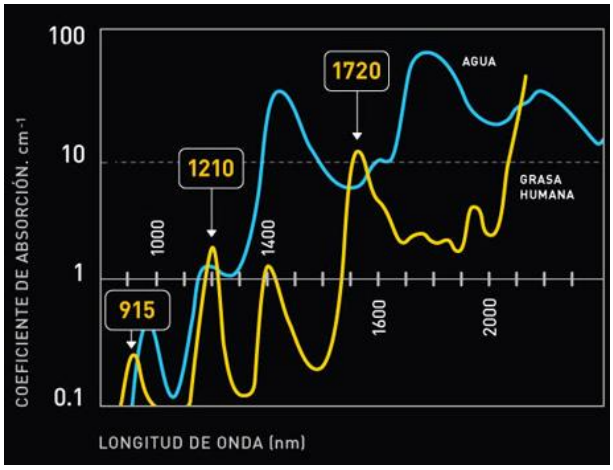

Figure 1. Absorption curves for water (blue) and human fat (yellow) as a function of the wavelength.

Aim of this work

The main aim of this work is to study the viability of Ho^{3+} doped YAS microspheres as thermal sensors. With this in mind, the shift on the WGM wavelengths of the three emission bands (660 nm, 760 nm and 1200 nm) of Ho^{3+} doped YAS microspheres were analysed with the temperature. A 532 nm continuous wave laser was used as the excitation source, producing the heating of the sample due to non-radiative processes in the de-excitation of the Ho^{3+} ions. Special attention has been paid to the 1200 nm emission band due to its interesting applications.

The specific objectives of this work are summarized as follows:

- To detect whispering gallery modes of a YAS microsphere doped with trivalent holmium ions.

- To find the dependence of the whispering gallery modes with the laser power, when the microsphere is excited with a laser.
- To find a temperature calibration to estimate the WGM wavelengths displacement for the holmium emission bands with temperature.
- To analyse which is the dominant optical property in the wavelength shift of the whispering gallery modes when a temperature change takes place.

Chapter 2. Theoretical background.

Ya que en esta sección se abordarán los fundamentos teóricos de los experimentos realizados en este trabajo, en primer lugar, se introducirán algunas de las propiedades del holmio, que pertenece al grupo de los lantánidos, y, a continuación, se profundizará en la teoría de los WGM en una microesfera. Todo ello sentará la base para el estudio de los desplazamientos de las longitudes de onda de estos modos resonantes cuando tiene lugar un aumento de la temperatura de la microesfera.

2.1 Holmium electronic structure and energy levels.

The microspheres involved in this work were doped with holmium ions. Holmium is an element that belongs to the chemical series of lanthanides. The electronic structure of this group of elements in their ground state consists on a series of complete layers with the same structure as xenon, plus the 4f layer partially filled. Ions from different lanthanides only differ in the number of electrons in the 4f shell, speaking in terms of electronic structure. Generally, these ions are trivalent and the ionisation process results in the removal of one 4f and two 6s electrons. The fluorescence emissions observed on lanthanides ions come from electronic transitions between levels of the 4f layer partially filled. The electrons initially at the 4f shell may absorb energy from the incident light and "jump" to unoccupied 4f levels. Specifically, holmium and its trivalent ion electronic configuration are [28]:

$$Ho\colon [Xe]4f^{11}6s^{2}$$

$$Ho^{3+}\colon [Xe]4f^{10}$$

where [Xe] denotes: $1s^2 2s^2 2p^6 3s^2 3p^6 3d^{10} 4s^2 4p^6 4d^{10} 5s^2 5p^6$.

As it was mentioned before, lanthanides are very interesting doping materials due to their emissions in the visible and near infrared region of the spectrum. Specifically, in this work we are interested in the following holmium transitions: $^5F_5 \rightarrow {}^5I_8$, $S_2\,(^5F_4) \rightarrow {}^5I_7$ and $^5I_6 \rightarrow {}^5I_8$. In Fig. 2 holmium energy levels with the transitions of interest are shown.

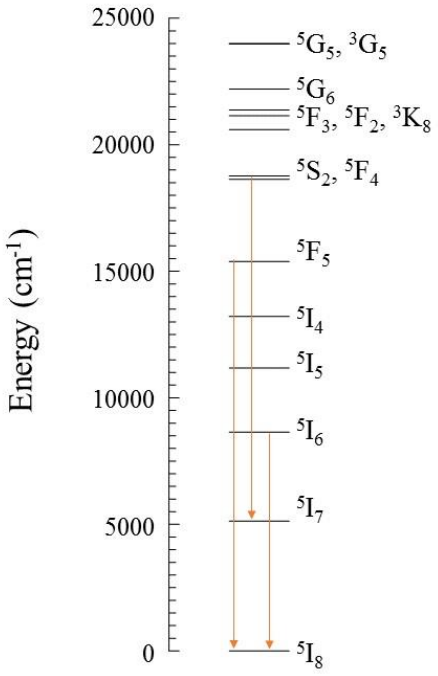

Figure 2. Partial energy-level diagram for holmium trivalent ions and most relevant transitions.

2.2 Whispering gallery modes in a microsphere.

To act as resonant cavities, microspheres are made of a transparent dielectric with a higher refractive index than the surrounding media, as it was said in the introduction. Light could be trapped inside the microsphere, producing a series of reflections on the sphere walls, some of them return to their starting point in phase, which causes a resonant effect. These resonances are the WGM. In Fig. 3 this resonant effect is shown, from a geometrical point of view.

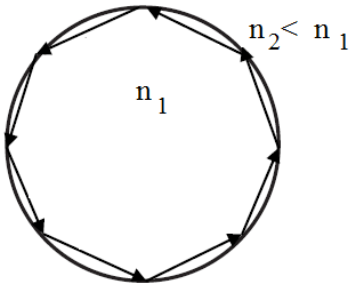

Figure 3. Multiple reflections inside a microsphere.

2.2.1 WGM resonator coupling.

It is important to have an adequate mechanism to couple light in and out the resonator, in this case the microsphere. There are three main types of light coupling methods: free wave coupling, fluorescent coupling and evanescent coupling [29].

- **Free wave coupling:**

This method is the least efficient of the three [30], since it is based on radiative exchange between radiating modes of the resonator and free space. It consists on exciting WGM inside the resonator illuminating it with outside light, and some of the WGM may leave the resonator into free space.

- **Evanescent coupling**:

This consists on placing a structure which has an optical evanescent field in the surroundings of the resonator, so the evanescent fields of the resonator and the coupler may overlap. The most used structure is a tapered optical fiber [30] that is notably thinned, through processes of heating and stretching (Fig. 4).

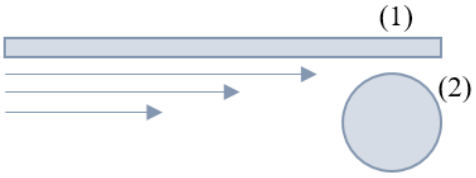

Figure 4. Scheme of the tapered optical fiber (1) and the microsphere (2).

The thickness of the tapered optical fiber forces light to focus to a diameter practically equal or less than its wavelength. The evanescent field may stretch so much that most of the beam optical power is really outside the fiber. Then, this evanescent field and the resonator evanescent field overlap and a highly efficient resonator-waveguide coupling takes place.

Although this method has been found highly efficient (coupling efficiencies of about 99.99% have been reached [30]), it has some disadvantages: an additional element is needed, and the tapered fibres are very fragile, lasting no longer than a day.

- **Fluorescent coupling:**

This is a simpler method than those described previously. In this case the microsphere is doped with some fluorescent substance. When excited by a short wavelength, the substance emits a broad spectrum that may get trapped inside the resonator [30].

In this work, Ho^{3+} doped YAS microspheres were used. When the doped microsphere is excited with a laser, the emission of the doping ions takes place. These emissions are shown on the spectrum as broad bands, but some of the emitted wavelengths could be trapped inside the microsphere. Then, sharp peaks, corresponding to the WGM, can be observed overlapping with the fluorescence emissions of the dopant ions. If the excitation radiation is located at the centre of the microsphere, and the detection is performed near its border, the WGM peaks will appear with the best visibility [31].

Fig. 5 shows an example of the spectrum obtained exciting a Er^{3+} and Yb^{3+} codoped glass and microsphere with a laser, obtained from Labrador-Páez *et al.* [12]. The emission spectrum is formed by the bulk glass spectrum and it is overlapped with a series of peaks associated with the resonant modes of the microsphere.

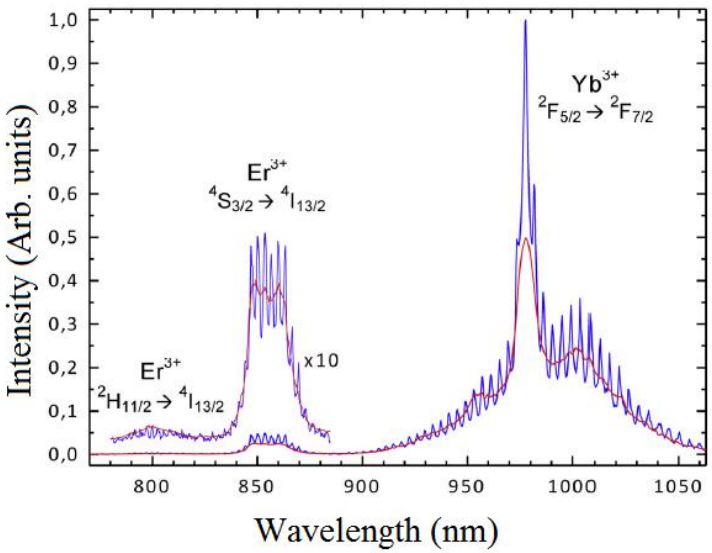

Figure 5. Emission spectra of a Yb^{3+}–Er^{3+} codoped glass (red line) and microsphere (blue line). In the range from 780 to 885 nm a zoom (×10) of the spectra was made. Obtained from Labrador-Páez *et al.* [12].

2.2.2 Resonance condition.

The WGM effect can be studied under a geometrical optics approximation, obtaining that the WGM must satisfy the following resonance condition [32]:

$$\frac{\lambda}{n} \cdot l = 2\pi R \tag{1}$$

with l the polar mode number, that is the number of wavelengths that fits into the resonator, n the microsphere refractive index and R its radius.

These resonant wavelengths can suffer shifts due to changes in the refractive index, or in the size of the cavity. Such changes on the microsphere parameters may occur because of temperature variations, among others. The derivative of the resonant wavelength with respect to temperature, provides a relationship between both parameters:

$$\frac{d\lambda}{dT} = \left(\frac{1}{n}\frac{\delta n}{\delta T} + \frac{1}{r}\frac{\delta r}{\delta T}\right)\lambda = (\beta + \alpha)\lambda \tag{2}$$

where $\beta = \frac{1}{n}\frac{\delta n}{\delta T}$, is the thermo-optic coefficient, and $\alpha = \frac{1}{r}\frac{\delta r}{\delta T}$, the thermal expansion coefficient. It is known that the sign of these coefficients is positive [33].Therefore, if a temperature increase takes place, the peaks corresponding to the resonant wavelengths in the emission spectrum of the microsphere will shift to the red region of the spectra. This effect is shown in Fig. 6, where the WGM displacement when the microsphere is excited and heated with a laser is represented.

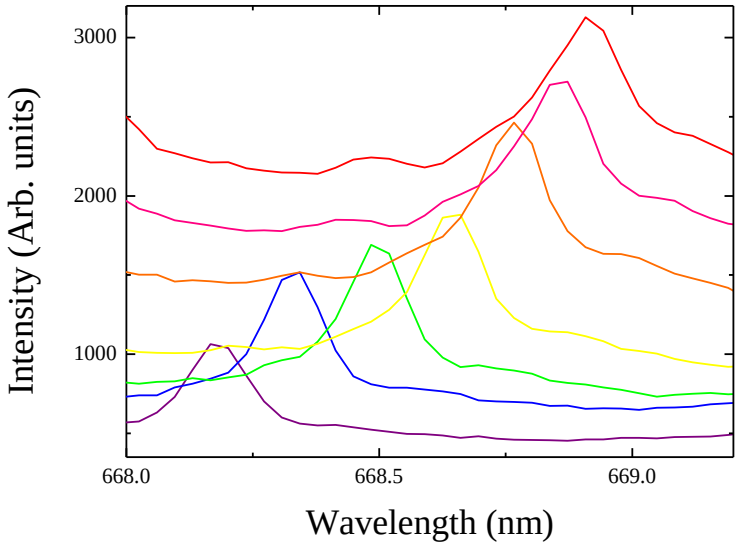

Figure 6. Displacement of the WGM peaks of a Ho^{3+} doped YAS microsphere due to the increase of the laser excitation power.

2.2.3 Microspheres parameters.

The main parameters that characterize the WGM are:

- **Quality factor:**

The quality factor (or Q-factor) of a resonator is defined as [34]:

$$Q = \omega_0 \frac{Stored\ energy}{Power\ loss} = \omega_0 \cdot \tau = \frac{\lambda}{\Delta\lambda} \tag{3}$$

where $\omega_0 = 2\pi\nu_0$ is the angular frequency, ν_0 the frequency of the resonance, τ is the cavity decay lifetime, λ is the resonant wavelength and $\Delta\lambda$ represents the observed line-width of the peaks. From Eq. (3) it can be deduced that the Q-factor is proportional to the time that energy is trapped inside the resonator, so for higher Q-factors energy last longer inside the resonator.

This parameter is often used to describe the resonator performance. A Q-factor is considered high when it is in the range from 10^3 up to 10^6, and ultra-high when it is over 10^7 [35].

- **Loss mechanisms:**

The intrinsic quality factor of a resonator gets contributions because of losses from multiple processes, the main contributions are the following [36]:

$$Q^{-1}{}_{int} = Q^{-1}{}_{mat} + Q^{-1}{}_{surf} \tag{4}$$

where Q_{mat} is related with the intrinsic material absorption (the resonator must be made with a high transparent material in order to $Q_{mat}^{-1} \approx 0$) and Q_{surf} represents the surface absorption losses and the surface scattering losses, intrinsic to the cavity surface, for example, surface imperfections or particles adhered to the surface.

- **Sensitivity:**

Optical temperature sensors are often characterized in terms of their sensitivity, which is a parameter that represents the variation of the measured variable with the temperature relative to its magnitude [18]:

$$S = \frac{1}{MP}\frac{dMP}{dT} \tag{5}$$

where MP is the measured variable.

Then, the sensitivity for the displacement of the WGM with temperature is:

$$S_{WGM} = \frac{1}{\lambda}\frac{d\lambda}{dT} \tag{6}$$

where $d\lambda/dT$ is given by Eq. (2).

- **Temperature resolution:**

On the other hand, the temperature resolution of the thermal sensor can be defined as [37]:

$$\Delta T_{\min WGM} = \frac{\Delta\lambda_{min}}{\lambda \cdot S_{WGM}} \tag{7}$$

where $\Delta T_{\min WGM}$ is the temperature resolution, which represents the minimum temperature variation that can be detected by a thermal sensor, $\Delta\lambda_{min}$ represents the resolution of the WGM peaks, λ the resonant wavelength and S_{WGM} the sensitivity.

Chapter 3. Methodology and experimental procedures.

En este capítulo se muestran los métodos y montajes experimentales utilizados en este trabajo. En primer lugar, se explicará la metodología seguida en los experimentos realizados. El objetivo de este trabajo es estudiar la viabilidad de utilizar una microesfera de YAS dopada con iones de Ho^{3+} como sensor de temperatura, para conseguir dicho objetivo, se realizaron dos tareas principales: una calibración de los desplazamientos de las longitudes de onda de los WGM con la temperatura obtenidos al calentar la microesfera y la medida de los desplazamientos cuando excitamos la microesfera con un láser y hacemos variar su potencia. En segundo lugar, se explican los procedimientos y montajes experimentales utilizados para realizar estas tareas.

3.1 Methodology.

When a microsphere is excited with a laser beam of known power, the microsphere temperature remains unknown. To estimate this temperature, and so use the microsphere as a sensor device, the emission spectrum of the WGM of the microsphere will be recorded in two experimental procedures.

The first one constitutes the temperature calibration and consists on heating the microsphere with a heater and recording the variations of the microsphere WGM while increases the temperature. As mentioned before, the spectrum presents a series of peaks, associated with the WGM, which will move to the red part of the spectrum with increasing values of the temperature. An analysis of the data will allow us to represent the displacements versus the measured values of temperature and obtain a relationship.

The second experimental procedure is the microsphere laser heating. The microsphere is excited by a laser, in what is named fluorescent coupling, and heated at the same time. The emission spectra are recorded for increasing values of the laser power,

and from this data the total displacement of the WGM peaks can be obtained. This value of the displacement can be introduced in the relationship obtained in the calibration process to obtain the temperature change undergone by the microsphere.

3.2 Experimental procedures.

3.2.1 Microspheres production.

Microspheres are good candidates as temperature sensors because of their cheap and easy production. They can be fabricated by different techniques as polishing, chemical etching and rapid quenching of liquid droplets [38]. The rapid quenching of liquid droplets is a widely used method. It consists on grinding a bulk sample into very small glass particles, then melting these particles and letting surface tension to pull the melted glass into spheres, that are quickly quenched [39].

The microspheres used in this experiment were produced by Prof. Vladimir N. Sigaev from D. I. Mendeleev Russian Chemical Technology University. These microspheres were obtained from a doped Ho^{3+} YAS glass, with the composition: Y_2O_3 (31.4 w%), Al_2O_3 (39.5 w%), SiO_2 (29.1 w%) and HoO_5 (7.8 w%) [39].

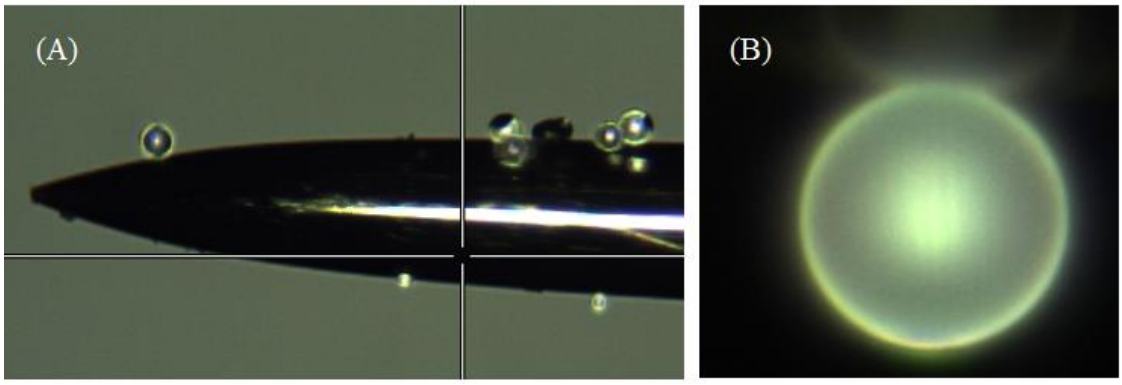

Figure 7. Optical image of a set of microspheres on a needle (A). Optical image of the main microsphere studied in this work, with a diameter about 27 μm (B).

3.2.2 Experimental setup.

The setup used in this work is shown in Fig. 8 (C) and consists of the following:

A 532 nm continuous wave Nd:YAG laser is placed in the optical system. The laser beam is diverted with a mirror (M1) to a pinhole (P) and a collimating lens (CL), to obtain a circularly collimated beam. Then, the light is reflected by a dichroic mirror (M2) to a microscope objective (MO), that focalizes the light in the microsphere. Between M2 and MO it is placed a beam splitter (BS) that sends part of the light to a CCD camera that shows an image of the microspheres on a TV screen. With this image, the microsphere can be placed wherever it is needed to focalize the laser beam on it. A long pass filter was used to avoid second harmonics. The light transmitted by the dichroic mirror is reflected by a high precision mirror (M3) and focused on:

i. The entrance slit of the spectrograph Andor SR-3031-B CCD Newton DU920N (Fig. 8 (A)): Used to obtain the microsphere emission spectrum on the visible region. A wavelength resolution of 0.11 nm can be reached with this instrument.
ii. An optical fiber (F) that is connected spectrograph Andor SR-500i-B2 InGaAs CCDDU490A-1.7 (Fig. 8 (B)): Used to obtain the microsphere emission spectrum on the near infrared region. This spectrograph has a wavelength resolution of 0.07 nm. In this case, the mirror M3 is removed so the light reaches the optical fiber.

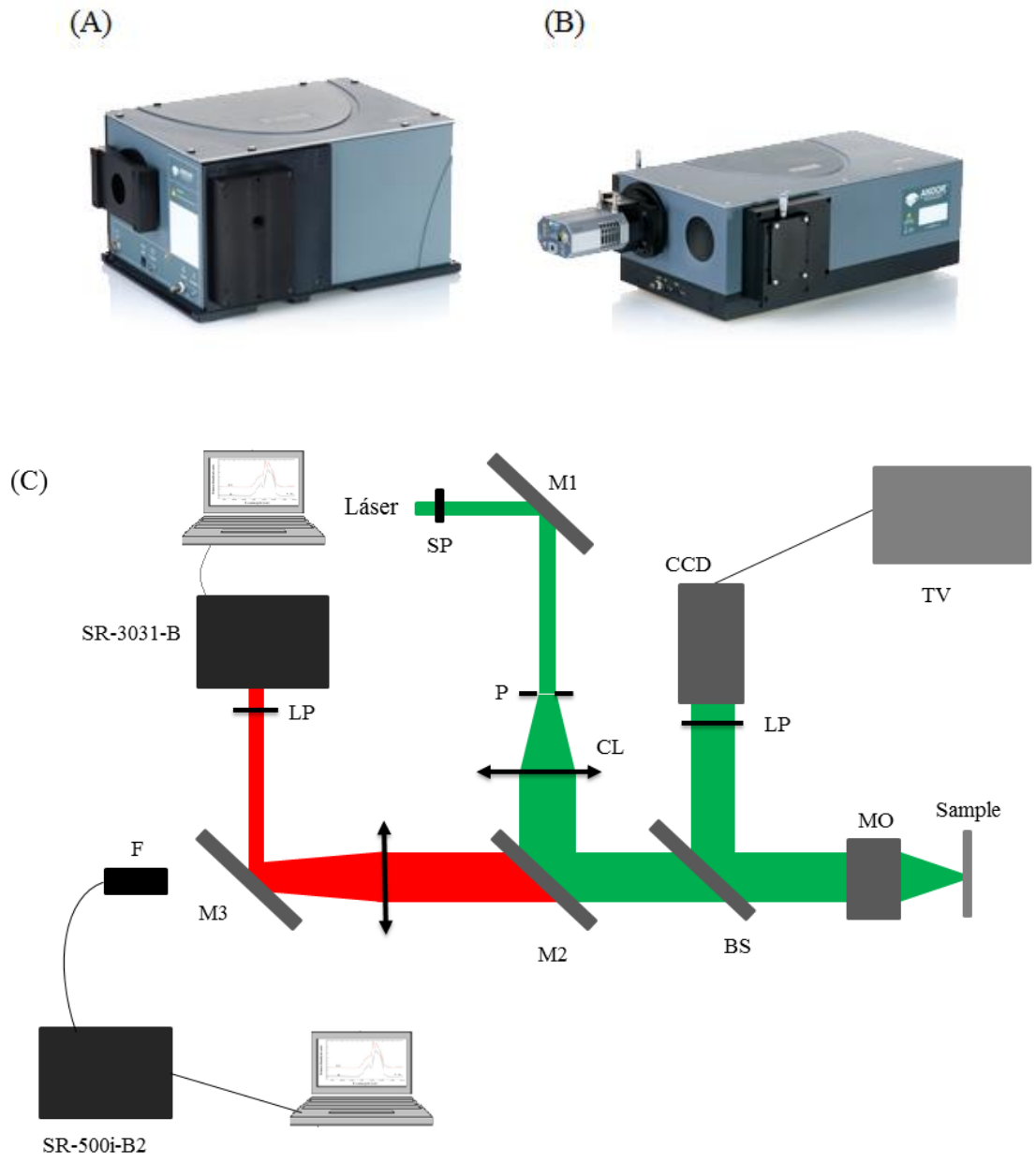

Figure 8. Spectrograph Andor SR-3031-B (A), Andor SR-500i-B2 (B), and experimental setup to obtain the emission spectrum of an excited microsphere (C).

Using this experimental setup, two taks were done:

i) **Temperature calibration:** To obtain the relationship between the temperature and the WGM wavelength displacement, a temperature calibration of a microsphere was done. In this case, the microsphere was heated with a heater, with the laser at a constant and low power. The heater

was placed inside the optical system and to monitor the temperature a thermocouple was used, placed as close to the microsphere as possible.

Gradually increasing the temperature of the system, the emission spectrum of the doped microsphere for each temperature was obtained. So, with these multiple spectra, the displacement of the WGM wavelengths with the temperature can be estimated.

ii) **WGM displacement by laser excitation:** In this part of the work, the emission spectra of the Ho^{3+} doped YAS microsphere for increasing laser powers were obtained and recorded, in order to measure the displacement of the WGM peaks for different laser powers.

Chapter 4. Results and discussion.

En este capítulo se presentan y analizan los resultados obtenidos en este trabajo. En primer lugar, se observan los modos de resonancia de una microesfera de YAS dopada con Ho^{3+}. Por un lado, se obtiene la anchura a mitad altura para estos picos de aproximadamente 0.2 nm y, por otro lado, se identifican las transiciones del holmio con las bandas de emisión observadas: $^5F_5 \rightarrow {}^5I_8$ (660 nm), $^5S_2$ ($^5F_4$) $\rightarrow {}^5I_7$ (760 nm) y $^5I_6 \rightarrow {}^5I_8$ (1200 nm). A continuación, se muestran los resultados de la calibración con la temperatura de una microesfera de aproximadamente 27 µm de diámetro, se obtienen las relaciones entre los desplazamientos de las longitudes de onda de los WGM y la temperatura de la microesfera para las tres bandas de emisión. Partiendo de la calibración con la temperatura, se encuentran desplazamientos promedios de 34.8, 40.1 y 62.2 pm/K para las bandas de emisión del holmio en 660, 760 y 1200 nm, respectivamente. Por otro lado, se obtienen desplazamientos promedios de 17.6 pm/mW, 20.85 pm/mW y 35.16 pm/mW cuando se calienta la microesfera con el láser. Se obtiene una resolución de temperatura de 0.03 K para las bandas en 660 y 760 nm, y de 0.01K para la de 1200nm. Finalmente, se encuentra que la causa dominante en los desplazamientos de los WGM debe ser el cambio en el índice de refracción, frente al cambio en el tamaño de la microesfera.

4.1 WGM in a microsphere.

The emission spectrum of a Ho^{3+} doped YAS microsphere obtained exciting with a laser power of 3mW at room temperature is shown in Fig. 9 (A), placing the excitation and the detection at the centre of the microsphere, three broad bands can be observed corresponding to typical transitions of the trivalent ion Ho^{3+}. The broad band centred at 660nm can be assigned to the holmium transition $^5F_5 \rightarrow {}^5I_8$, the one at 760 nm to $^5S_2$ ($^5F_4$) $\rightarrow {}^5I_7$, and the 1200nm band to $^5I_6 \rightarrow {}^5I_8$. If the detection is placed at the microsphere border, the WGM are observed overlapping the holmium emission bands, as can be seen in Fig. 9 (B).

It is interesting to note that the relative intensities of the emission bands are not the same in both spectra. It can be explained in basis to radiative transfer that produces a reduction of the $^5F_5 \rightarrow {}^5I_8$ emission band respect to the $^5S_2(^5F_4) \rightarrow {}^5I_7$ band.

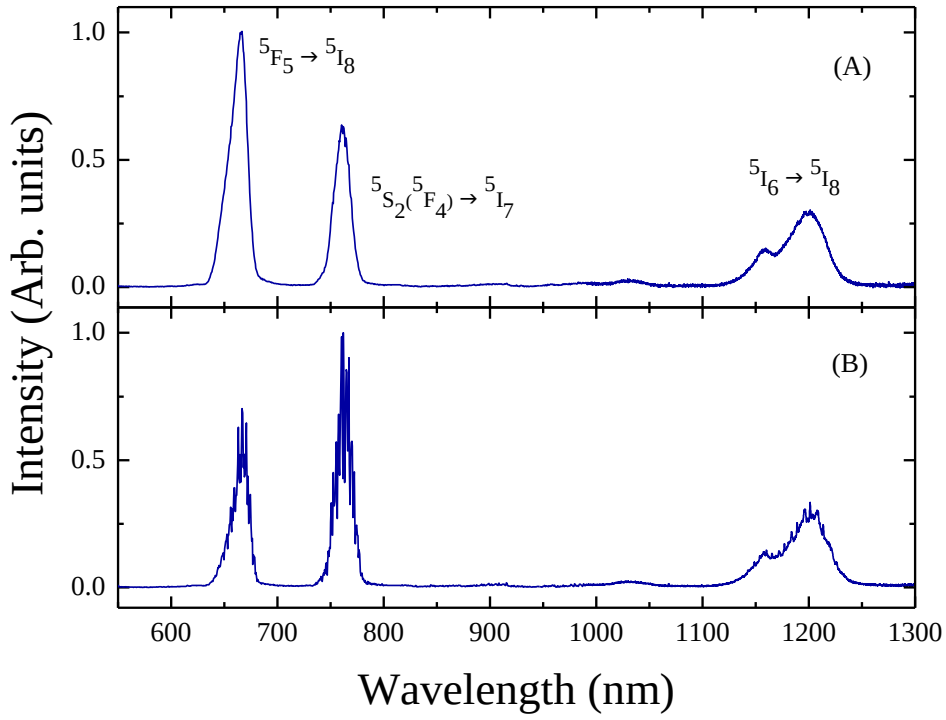

Figure 9. (A) Emission spectrum of a Ho^{3+} doped YAS microsphere obtained under excitation at 532nm at room temperature, placing the detection at its centre (showing the corresponding transitions). (B) Emission spectrum of a Ho^{3+} doped YAS microsphere showing the WGM under excitation at 532nm at room temperature, placing the detection at the border of the microsphere.

In Fig. 10, the emission centred in 660 nm is presented, showing in more detail the typical sharp peaks associated to the WGM. The full width at half maximum (FWHM) found was 0.23 nm, obtained by fitting the peak to a Gaussian function.

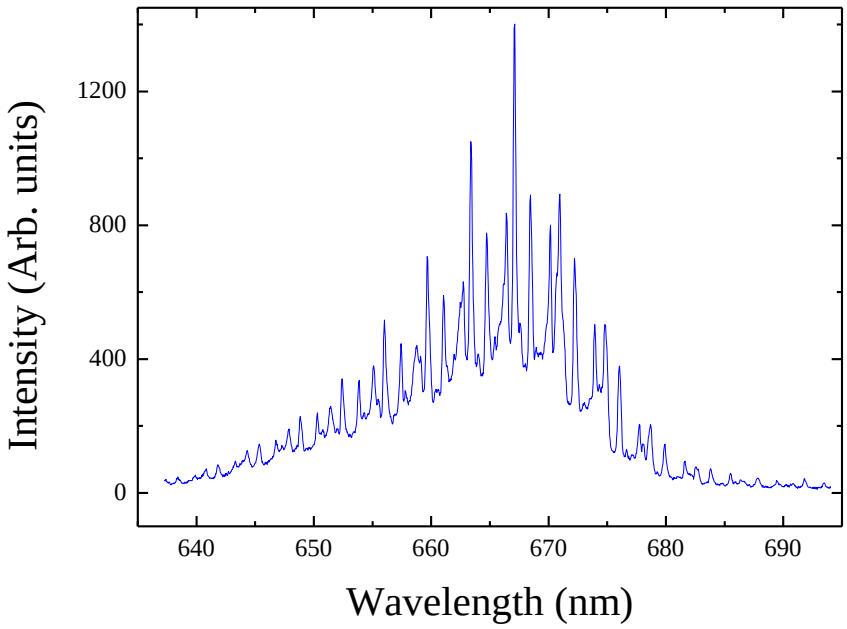

Figure 10. Emission band centred at 660 nm of a Ho^{3+} doped YAS microsphere showing the WGM.

4.2 Temperature calibration.

The shift in the WGM peaks of a Ho^{3+} doped YAS microsphere of about 27 μm of diameter, when it is heated with a heater, was obtained to do a temperature calibration. The temperature was increased from 20.6 to 32.3ºC and the corresponding spectra for different temperatures in that range were recorded. From these spectra, the most sharp and defined WGM peaks for different wavelengths were selected for the emission band centred at 660 nm, and the displacements of their maxima for each temperature were estimated.

Fig. 11 presents the average wavelength displacement of the WGM peaks of the 660 nm band, showing a linear dependence. For a temperature increase of 11.7 degrees, the WGM peaks under study shifted an average of 0.41 nm. From these data, the relationship between the wavelength displacement and the temperature can be obtained by linear fitting. This calibration makes possible to estimate the temperature value

reached with the laser heating that will be presented in the following section. The results of the linear fitting are shown in Table 1.

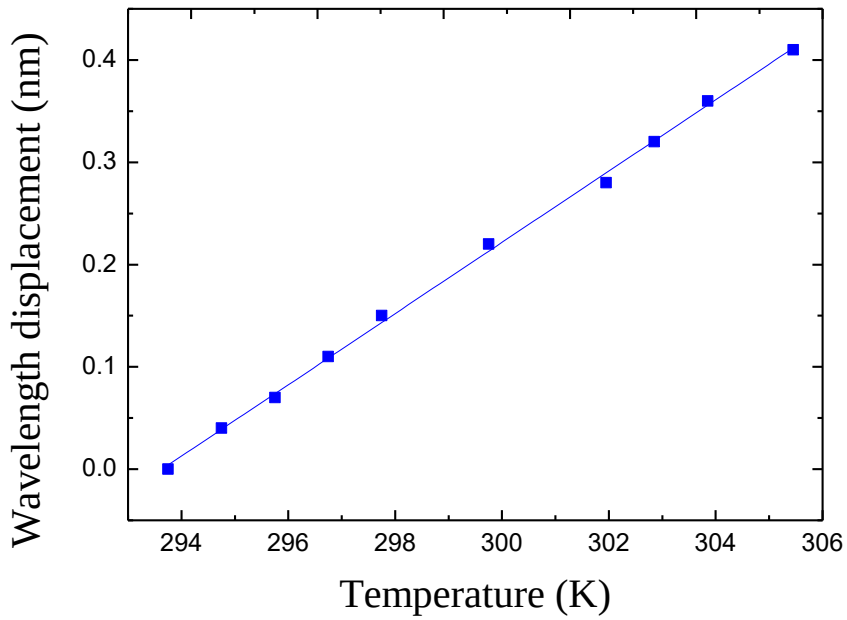

Figure 11. Displacement of the WGM peaks at the 660 nm emission of a Ho^{3+} doped YAS microsphere as a function of temperature.

Considering Eq.(2) and the temperature calibration for the 660 nm emission band experimentally obtained, the relationship between the WGM peaks displacement and the temperature for the 760 nm and the 1200 nm emission bands can be inferred, in a pseudo-experimental way. The dependences are shown in Table 1 and the results represented in Fig. 12. For a temperature increase of 11.7 K, shifts of approximately 0.47 nm and 0.75 nm are predicted for the 760 nm and 1200 nm emission bands, respectively.

Table 1. Linear fit parameters ($\Delta\lambda = a \cdot T + b$) for the 660 nm emission band and predicted parameters for the 760 nm and 1200 nm bands.

	660 nm band	**760 nm band**	**1200 nm band**
Slope: a (nm/K)	0.0348	0.0401	0.0633
Intercept: b (nm)	-10.2271	-11.7765	-18.5928

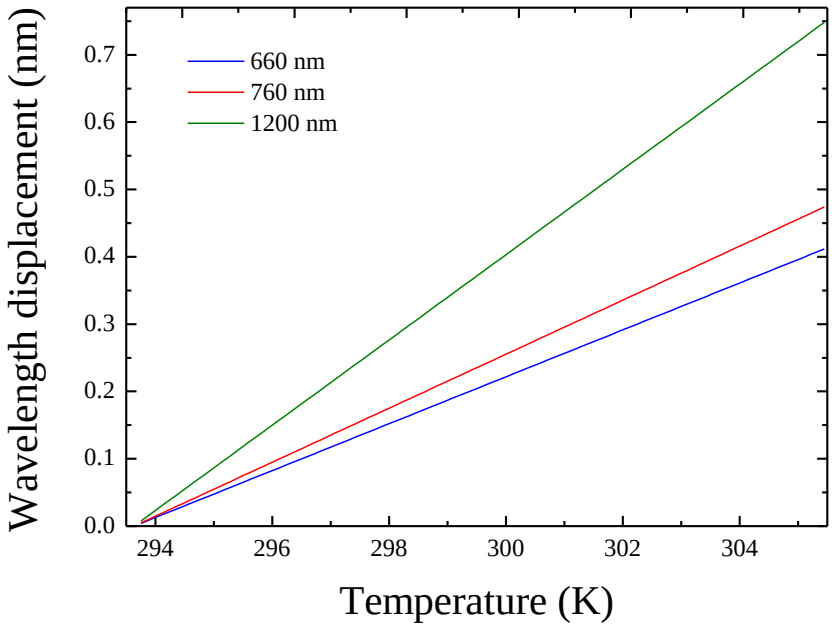

Figure 12. Displacement of the WGM wavelengths for the three emission bands for a Ho^{3+} doped microsphere.

The slopes shown in table 1 (34.8 pm/K, 40.1 pm/K and 63.3 pm/K), represent the variation of the displacement of the WGM peaks with temperature. As can be observed in Fig. 12, the slope increases for increasing values of the central wavelength of the emission band. Considering the results for WGM displacements with temperature in microspheres obtained in other experiments [12, 18], it can be seen that, a larger displacement of the WGM peaks, up to six times greater, has been obtained for the Ho^{3+} doped YAS microspheres.

4.3 WGM displacement due to laser power.

Once the WGM in the microsphere were detected and the temperature calibration was done, the next step is to increase the laser power, to see how it affects the wavelengths of the resonant modes. In this part of the work, the laser power was gradually increased up to a value of 64 mW, and the successive spectra were recorded and processed to obtain the displacement of the WGM peaks with the temperature.

Four WGM peaks were selected for each one of the three emission bands considered and their displacements with the laser power were estimated by analysing the recorded spectra. The results are presented in Fig. 13, showing that, increasing the laser power from 3 to 64 mW, average displacements of 1.07±0.04 nm, 1.20±0.04 nm and 2.10±0.07 nm are found for the emission bands centred at 660 nm, 760 nm and 1200 nm, respectively, under the same measurement conditions. A shift to the red region of the spectrum is observed, as predicted with Eq.(2).

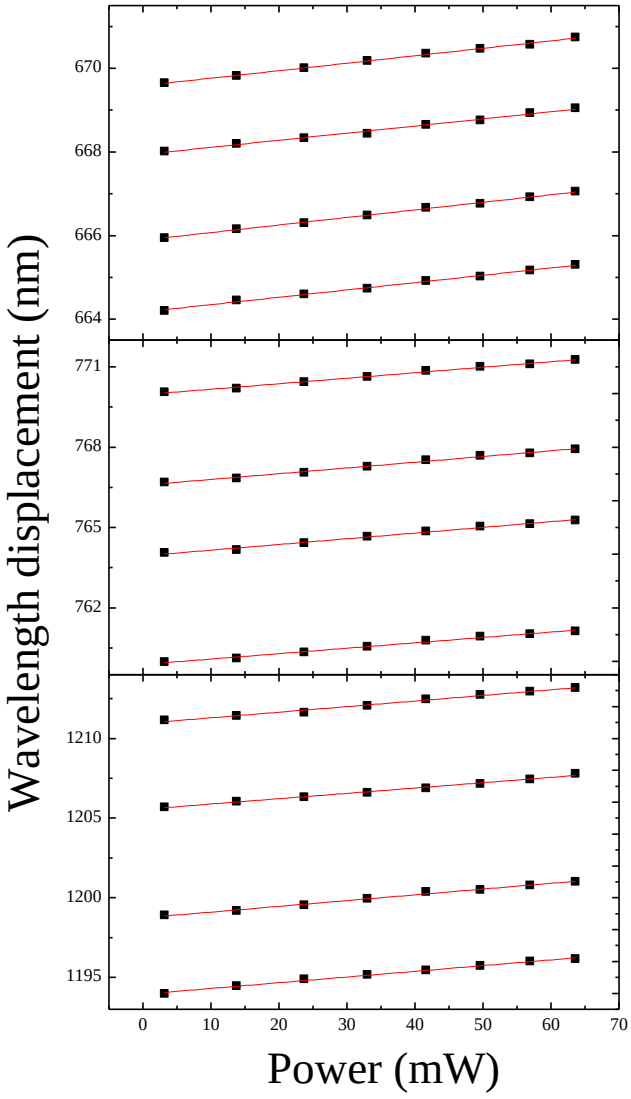

Figure 13. Displacement of the WGM peaks at the three emissions of a Ho^{3+} doped YAS microsphere (with a diameter of 27μm) as a function of the laser power.

From Fig. 13, average displacement rates of 17.6 pm/mW, 20.85 pm/mW and 35.16 pm/mW were found, for the emission bands centred at 660 nm, 760 nm and 1200 nm, respectively. The greatest rate corresponds to the peaks at the 1200 nm emission band. The displacement of the WGM increases with the wavelength of the emission band, behaviour that can be inferred from Eq.(2).

Fig. 14 shows the WGM displacement rate with the laser power as a function of the resonant wavelength. The relationship between the displacement rate of the WGM wavelengths with both the laser power and the wavelength seems to be linear.

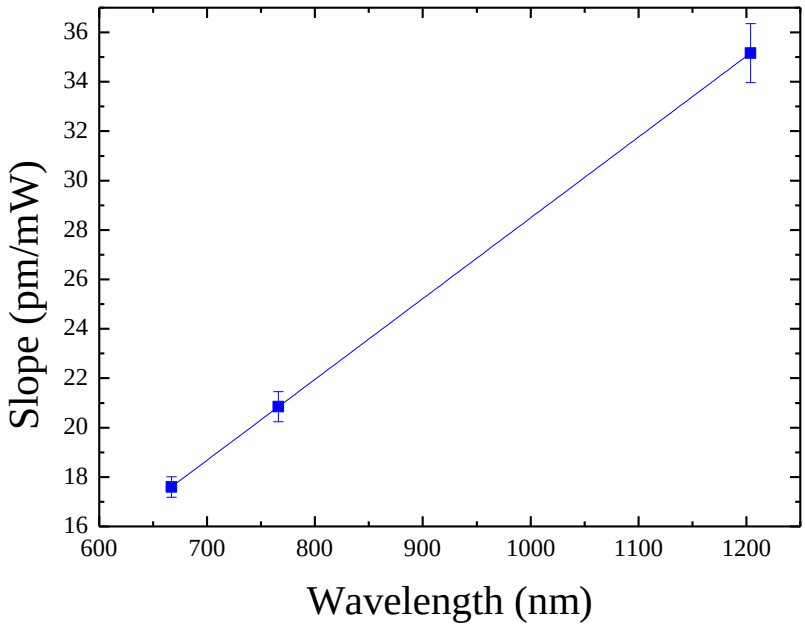

Figure 14. WGM resonances displacement with laser power for the three emission bands (blue squares). The solid line corresponds to a linear fitting (blue line).

As an example, let us consider the average WGM displacement of the 660 nm centred band obtained with the laser excitation of the Ho^{3+} doped YAS microsphere, which is 1.07 nm. Using the temperature calibration obtained for this microsphere for the mentioned band (see linear fit parameters in Table 1), the temperature reached with the laser can be estimated, obtaining a value of 324.6 K (51.6 ºC).

On the other hand, WGM displacements of 1.20 nm and 2.10 nm were obtained experimentally with the laser excitation for a temperature of 324.6 K, for the 760 nm and 1200 nm bands, respectively. These values can be predicted by using the pseudo-experimental relationships between the WGM displacement and the temperature described in Table 1, using the estimated value of temperature previously obtained for the 660 nm band (T = 324.6 K), displacements of 1.24 nm and 1.95 nm are found, in good agreement with the experimental values above. It can be concluded that with this method, the temperature of a Ho^{3+} doped YAS microsphere can be estimated using different emission bands, studying the WGM wavelengths displacement when it is heated.

Sensitivity and temperature resolution:

The sensitivity of the WGM wavelength displacement was calculated with Eq. (6), the results are shown in Fig. 15.

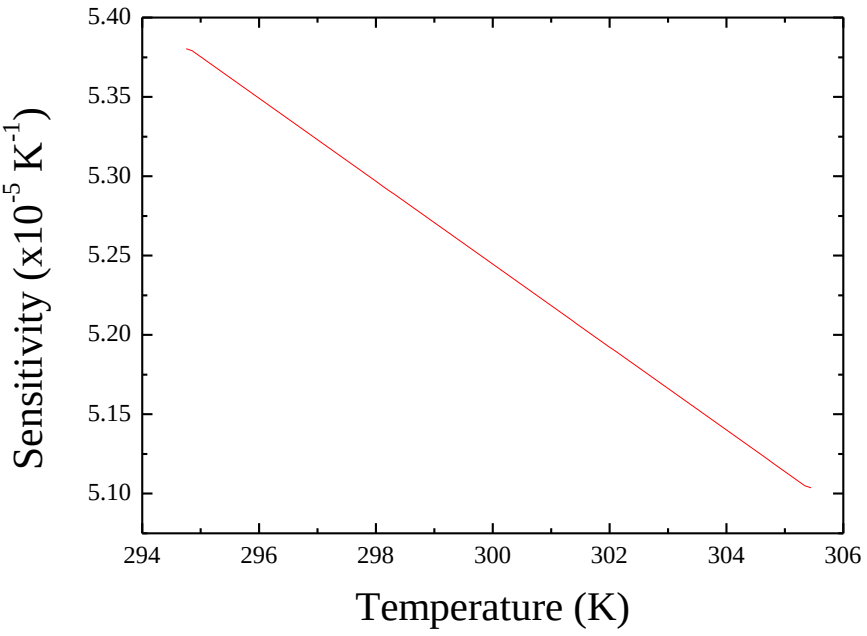

Figure 15. Sensitivity for the displacement of the WGM wavelength, using Eq. (6)

The sensitivity of the WGM displacement reaches its maximum for the lowest temperature at the 660 nm band, $S_{WGM\ max} = 5.38 \cdot 10^{-5}\ K^{-1}$. Moreover, considering that the WGM limit of detection is about 1% of the line-width of the resonance [40], and that the

wavelength resolution that can be reached with the instrument used is 0.11 nm, using Eq.(7), the temperature resolution of this method is $\Delta T_{\min WGM} = 0.03$ K for the 660 nm and the 760 nm centred bands. On the other hand, the instrument used for the 1200 nm band has a wavelength resolution of 0.07 nm, then for this band: $\Delta T_{\min WGM} = 0.01\ K$. These values are similar to the one found in Ref [12].

Coefficient of thermal expansion and refractive index:

When a temperature change takes place, there is a variation in the size of the microsphere and in the refractive index. We will here analyse the relative contribution of both parameters to the WGM shifts.

Since the coefficient of thermal expansion of these microspheres is unknown, we will use the one obtained from Hyatt [41] for a glass with a similar chemical composition to the one used in this work: YAS-10, Y_2O_3 (35 w%), Al_2O_3 (35 w%), SiO_2 (30 w%), which is $\alpha=48\cdot10^{-7}$ $^oC^{-1}$. Introducing this value for α in Eq. (2), the contribution of the thermal expansion coefficient to the WGM wavelength shift is obtained and shown in Fig. 16, together with the experimental displacement. Comparing both, the total displacement and the displacement associated to the thermal expansion, it can be concluded that the major contribution to the peaks displacement comes from the thermo-optic coefficient. Therefore, the contribution of the thermo-optic coefficient can be extracted from Fig. 16, and a value the thermo-optic coefficient of $\beta \approx 5.31\cdot10^{-5}$ K^{-1} is estimated. This value is an order of magnitude greater than thermo-optic coefficients found for other glasses [42].

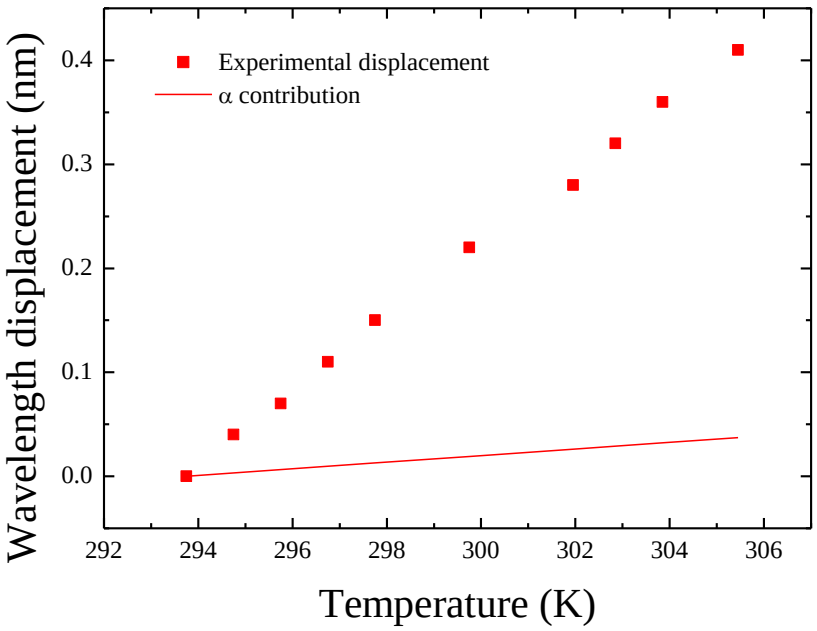

Figure 16. Experimental displacement of the WGM with temperature at the 660 nm emission band (red squares). Contribution of the thermal expansion coefficient obtained from Hyatt to the WGM displacement of a Ho^{3+} doped YAS microsphere (red line).

Chapter 5. Conclusions and future projects.

Conclusions.

The transitions of the trivalent holmium ions: $^5F_5 \rightarrow {}^5I_8$, $^5S_2\,(^5F_4) \rightarrow {}^5I_7$ and $^5I_6 \rightarrow {}^5I_8$ were identified in the Ho^{3+} doped YAS microsphere emission spectrum when it is excited with a 532 nm laser, corresponding to the broad bands centred at 660 nm, 760 nm and 1200 nm, respectively.

Whispering gallery modes, as emission sharp peaks, were observed in the Ho^{3+} doped YAS microsphere emission spectrum, when the excitation was performed in the microsphere centre and the detection placed in its border.

The temperature calibration was made for the emission band centred at 660 nm, and the relationships between the WGM peaks displacement and the temperature for the 760 nm and the 1200 nm emission bands were inferred, in a pseudo-experimental way. Displacement rates of the WGM peaks with temperature of 34.8 pm/K, 40.1 pm/K and 63.3 pm/K were found for each emission band (660 nm, 760 nm and 1200 nm), respectively.

Moreover, the consequences of heating a microsphere with a 532 nm laser were analysed. Increasing the laser power from 3 to 64 mW, average displacements of 1.07 nm, 1.20 nm and 2.10 nm were found for the emission bands centred at 660 nm, 760 nm and 1200 nm, respectively, under the same conditions. The red-shift of the positions of the peaks was observed. Average displacement rates of the WGM peaks with the laser power of 17.6 pm/mW, 20.85 pm/mW and 35.16 pm/mW were found, for each emission band respectively. We have found that the temperature resolution of this method is 0.03K for the bands centred in 660 y 760 nm, and 0.01K for the 1200 nm band.

Considering the results of the temperature calibration and the displacements under laser excitation, it was estimated that a temperature of about 324.6 K was reached due to laser heating.

Finally, it was concluded that the major contribution to the WGM peaks displacement comes from the thermo-optic coefficient, and that the thermal expansion coefficient hardly affects the displacement.

Taking all the results into account, it can be concluded that when a calibrated Ho^{3+} doped YAS microsphere is excited and heated up with a laser, its temperature can be estimated by studying the WGM peaks displacement. It is interesting to mention that the emission band centred at 1200 nm has medical applications, since that emission lays in the second biological window, where the biological tissues are partially transparent.

Future projects.

On the one hand, making an experimental temperature calibration for the 760 nm and the 1200 nm holmium emission bands would be interesting, since in this work only the 660 nm band was calibrated experimentally due to the lack of time. Moreover, trying other ways to calibrate the Ho^{3+} doped YAS microspheres would be helpful to corroborate the results obtained in this work.

On the other hand, a future experiment related to this work may consist of studying the penetration depth of the emission band centred at 1200 nm for the holmium ions in human tissue. To imitate the human tissue a phantom tissue could be used. This experiment may be useful to evaluate the possible medical applications of Ho^{3+} doped microspheres.

References

[1] W. Yoshiki, A. Chen-Jinnai, T. Tetsumoto, and T. Tanabe, “Observation of energy oscillation between strongly coupled counter-propagating ultra-high Q whispering gallery modes,” Opt. Express 23, 30851–30860 (2015).

[2] G. Lin, S. Diallo, R. Henriet, M. Jacquot, and Y.K. Chembo, “Barium fluoride whispering-gallery-mode diskresonator with one billion quality-factor,” Opt. Lett. 39, 6009–6012 (2014).

[3] A. B. Matsko, A. A. Savchenkov, D. Strekalov, V. S. Ilchenko, and L. Maleki, “Review of Applications of Whispering-Gallery Mode Resonators in Photonics and Nonlinear Optics,” IPN Progress Report 42- 162, pp. 1–51. (2005).

[4] A. B. Matsko and V. S. Ilchenko. “Optical resonators with whispering-gallery modes-Part I: Basics.” IEEE Journal of Selected Topics in Quantum Electronics Vol. 12, pp. 3-14. (2006)

[5] L. Rayleigh, "Further applications of Bessel's functions of high order to the whispering gallery and allied problems", Phil. Mag., vol. 27, pp. 100-109. (1914).

[6] L. Rayleigh, "The problem of the whispering gallery", Phil. Mag., vol. 20, pp. 1001-1004. (1910).

[7] P. Debye, "Der lichtdruck auf kugeln von beliebigem material", Ann. Phys., vol. 30, pp. 57-136. (1909).

[8] G. Mie, "Beitrage zur optik truber medien", Ann. Phys., vol. 25, pp. 377-445. (1908).

[9] C. G. B. Garrett, W. Kaiser, W. L. Bond, "Stimulated emission into optical whispering gallery modes of spheres", Phys. Rev., vol. 124, pp. 1807-1809. (1961).

[10] A. Ashkin, J. M. Dziedzic, "Observation of optical resonances of dielectric spheres by light scattering", Appl. Opt., vol. 20, pp. 1803-1814. (1981).

[11] P. Chyek, V. Ramaswamy, A. Ashkin, J. M. Dziedzic, "Simultaneous determination of refractive index and size of spherical dielectric particles from light scattering data", Appl. Opt., vol. 22, pp. 2302-2307. (1983).

[12] L. Labrador-Páez, C. Pérez-Rodríguez, I. R. Martín and S. Ríos. “Temperature response of the Whispering Gallery Mode resonances from the green upconversion emission of an Er3+–Yb3+ co-doped microsphere”. Laser Phys. Lett., 12 (2015).

[13] M. Horn and G. Schweiger. “Optical Temperature Sensor Based on Whispering Gallery Modes”. Ruhr-Universität Bochum. (2005).

[14] G. N. Atroshchenko and V. N. Sigaev. “Glassy microspheres and their applications in nuclear medicine (review)”. Glass and Ceramics. Vol. 72 397 – 404 (2016).

[15] L. Yang and K. J. Vahala, "Gain functionalization of silica microresonators," Opt. Lett. 28, 592-594. (2003).

[16] G. Miaomiao, W. Cong, L. Xianqing, L. Yuan, H. Fengqin and S. Z. Yong. “Controlled assembly of organic whispering-gallery-mode microlasers as highly sensitive chemical vapor sensors.” Chem. Commun., 53, 3102. (2017).

[17] V. K. Rai, “Temperature sensors and optical sensors,” Appl. Phys. B 88(2), 297–303 (2007).

[18] L. L. Martín, C. Pérez-Rodríguez, P. Haro-González, and I. R. Martín. “Whispering gallery modes in a glass microsphere as a function of temperature. Optics Express, 19, 25792-25798. (2011).

[19] M. B. Bortot, S. Prastalo and M. Prado. “Production and Characterization of Glass Microspheres for Hepatic Cancer Treatment.” Procedia Materials Science, 1, 351-358. (2012).

[20] L. Hench, D. Day, W. Höland and V. Rheinberger. “Glass and medicine.” International Journal of Applied Glass Science 1, 1, 104-117. (2010).

[21] J.-C.G. Bünzli. “Lanthanide Luminescence for Biomedical Analyses and Imaging.” Chem. Rev. 110, 2729–2755 (2010).

[22] T. Schweizer, B. N. Samson, J. R. Hector, W. S. Brocklesby, D. W. Hewak, D. N. Payne. "Infrared emission from holmium doped gallium lanthanum sulphide glass". Infrared Physics & Technology, 40, 329-335. (1999).

[23] U. Rocha, K. U. Kumar, C. Jacinto, I. Villa, F. Sanz-Rodríguez, M. C. Iglesias-de-la-Cruz, A. Juarranz, E. Carrasco, F. C. J. M. van Veggel, E. Bovero, J. García-Solé, and D. Jaque. “Neodymium-Doped LaF 3 Nanoparticles for

Fluorescence Bioimaging in the Second Biological Window.” Small. 10, 6, 1141–1154. (2014).

[24] Ol. Savchuk, J. J. Carvajal, L. G. De la Cruz, P. Haro-González, M. Aguiló and F. Díaz. “Luminescence thermometry and imaging in the second biological window at high penetration depth with Nd:KGd(WO4)2 nanoparticles.” J. Mater. Chem. C, 4, 7397. (2016).

[25] P. Vijayaraghavan, C. Liu, R. Vankayala, C. Chiang, K. C. Hwang. “Designing Multi-Branched Gold Nanoechinus for NIR Light Activated Dual Modal Photodynamic and Photothermal Therapy in the Second Biological Window.” Advanced Materials, 26, 6689–6695. (2014).

[26] Avijit Pramanik, Suhash Reddy Chavva, Zhen Fan, Sudarson Sekhar Sinha, Bhanu Priya Viraka Nellore, and Paresh Chandra Ray. “Extremely High Two-Photon Absorbing Graphene Oxide for Imaging of Tumor Cells in the Second Biological Window”. J. Phys. Chem. Lett., 5 (12), pp 2150–2154. (2014).

[27] E. Navarro-Cerón, D. H. Ortgies, B. del Rosal, F. Ren, A. Benayas, F. Vetrone, D. Ma, F. Sanz-Rodríguez, J. García-Solé, D. Jaque and E. Martín-Rodríguez. “Hybrid Nanostructures for High-Sensitivity Luminescence Nanothermometry in the Second Biological Window.” Advanced Materials, 27, 4781–4787. (2015).

[28] W. Koechner and M. Bass. “Solid-State Lasers: A Graduate Text”. Springer. (2003).

[29] M. Gomilšek, “Whispering Gallery Modes”, University of Ljubljana, Ljubljana, Seminario, (2011).

[30] Matsko, A.B., Savchenkov, A.A., Strekalov, D., Ilchenko, V.S. & Maleki, L. “Review of applications of whispering-gallery mode resonators in photonics and nonlinear optics.” (2005).

[31] L. L. Martín, P. Haro-González, I. R. Martín, D. Navarro-Urrios, D. Alonso, C. Pérez-Rodríguez, D. Jaque and N. E. Capuj. “Whispering-gallery modes in glass microspheres: optimization of pumping in a modified confocal microscope”. Opt. Lett. 36 615–7. (2011).

[32] T. Ioppolo, N. Das, and M. Volkan Ötügen. ”Whispering gallery modes of microspheres in the presence of a changing surrounding medium: A new ray-tracing analysis and sensor experiment” J. Appl. Phys. 107. 103105. (2010).

[33] D. S. Sanditov and B. S. Sydykov. “Modulus of elasticity and thermal expansion coefficient of glassy solids”. Phys. Solid State. 56 1006–8. (2014).

[34] Tobing, L. & Dumon, P. “Fundamental Principles of Operation and Notes on Fabrication of Photonic Microresonators.” Photonic Microresonator Research and Applications 156, 1-27 (2010).

[35] Vahala, K.J. Optical microcavities. Nature 424, 839-846 (2003).

[36] Kippenberg, T.J.A. Nonlinear optics in ultra-high-Q whispering-gallery optical microcavities. (2004).

[37] Q. Ma, T. Rossmann, and Z. Guo, “Temperature sensitivity of silica micro-resonators,” J. Phys. D Appl. Phys.41(24), 245111 (2008).

[38] G. R. Elliott, D. W. Hewak, G. S. Murugan, and J. S. Wilkinson, “Chalcogenide glass microspheres; their production, characterization and potential,” Opt. Express 15(26), 17542–17553 (2007).

[39] G. N. Atroshchenko and V. N. Sigaev. “Glassy microspheres and their applications in nuclear medicine (review)”. Glass and Ceramics. Vol. 72 397 – 404 (2016).

[40] F. Vollmer and S. Arnold, “Whispering-gallery-mode bio sensing: label-free detection down to single molecules”. Nat. Methods **5**(7), 591–596 (2008).

[41] M J Hyatt. Glass Properties in the Ytria-Alumina-Silica System. Journal of the American Ceramic Society, 70, 283-287. (1987).

[42] G. Ghosh. “Model for the thermo-optic coefficients of some standard optical glasses.” Journal of Non-Crystalline Solids 189, 191-196. (1995).